Measurement of Thin Film Isotropic and Anisotropic Thermal Conductivity Using 3ω and Thermoreflectance Imaging

K. Maize[1], Y. Ezzahri[2], X. Wang[3] and A. Shakouri[4]
Department of Electrical Engineering, University of California Santa Cruz
1156 High Street, Santa Cruz, California 95064-1077, USA
[1] kerry@soe.ucsc.edu
[2] younes@soe.ucsc.edu
[3] wangxi@soe.ucsc.edu
[4] ali@soe.ucsc.edu

Abstract

The 3ω method is a well established technique for experimentally extracting thermal conductivity of thin films and substrates. The 3ω method calculates thermal conductivity by measuring thin film temperature response to a metal strip heater deposited on the material's surface. The electrical resistance of the metal strip is used as both heat source and temperature sensor. An important factor in the accuracy of 3ω measurements is the fact that current should be confined to the thin film metal and any current leakage to the substrate will invalidate the results. This is because the heat source would not be localized on the surface anymore and also because any Schottky behavior at metal/semiconductor interface will create nonlinearities that affect the 3ω signal substantially. These problems are especially important at high temperatures where thermionic emission of electrons through oxide insulation layer becomes important. In this paper we propose thermoreflectance imaging as an additional method to determine thermal conductivity of thin film materials. Because thermoreflectance measures temperatures optically, the method is not as sensitive to the electrical properties of the metal heater. In addition, the temperature profile near the heat source can be used to make sure that there is no defect in the thin film metal heater. Theory is presented demonstrating thermoreflectance can also be used to measure anisotropic in-plane and cross-plane thermal conductivity in thin films. Preliminary thermoreflectance measurements were analyzed at various locations on the surface of isotropic, InGaAs thin film 3ω test samples. Experimental results are in agreement with simulated temperature distributions.

Keywords

Thermal conductivity, isotropy, anisotropy, thin film, superlattice, 3ω method, Thermoreflectance Imaging method.

1. Introduction

The 3ω technique has become standard in measuring thin film thermal conductivity [1, 4]. The method works by measuring heat diffusion into a material resulting from a sinusoidal heat source. Three-ω was motivated by a fundamental problem of DC thermal conductivity measurement at room temperature, in which a significant fraction of the heat that is intended to flow through the solid instead radiates out of the sample. Because the 3ω method is an AC technique, heat loss due to radiation is negligible at sufficient excitation frequency. The 3ω method has proven to be very versatile. It is capable of measuring thermal conductivity for samples of varying layer configuration and can also extract anisotropic thermal conductivities in materials with different cross-plane and in-plane thermal components [4].

We propose thermoreflectance as alternate method for measuring thermal conductivity in thin films. Because the thermoreflectance method uses the same fundamental governing heat equations as the 3ω method, it offers similar application to measuring both multilayer and anisotropic thermal conductivity. Thermoreflectance offers several advantages over the 3ω method. Thermal images provide instant, detailed, two-dimensional thermal maps of both the heat source and surrounding thin film surface. Any nonuniformity in the heating element or other thermal anomalies are immediately evident in the thermal image. These nonuniform components may not be detectable from electrical measurements alone using the 3ω method. Another advantage of thermoreflectance is that measurement of anisotropic thermal conductivity can theoretically be performed using a single heat source. In comparison, 3ω methods for measuring anisotropy require depositing two heat sources of different widths [4] and there are limitations in the minimum film thickness that can be analyzed.

2. Theoretical background

2.1. Surface temperature profile for an isotropic thin film on a semi-infinite isotropic substrate

A schematic diagram of the first test structure used in this study is shown in figure 1. The sample, originally configured for 3ω analysis, is comprised of a two micron InGaAs thin film semiconductor on top of a thermally thick InP substrate. They are separated by a 100 nm InAlAs buffer layer. The metal heater strip is deposited on top of the structure and electrically isolated from the thin film by a 185 nm SiO_2 layer.

In both methods the heater is excited by an AC current of frequency ω. The 3ω method uses the average temperature across the width of the heater to extract the thermal conductivity of the underlying thin film. With the thermoreflectance technique, we instead examine the thin film surface temperature distribution along a line extending perpendicular to the heater's long axis.

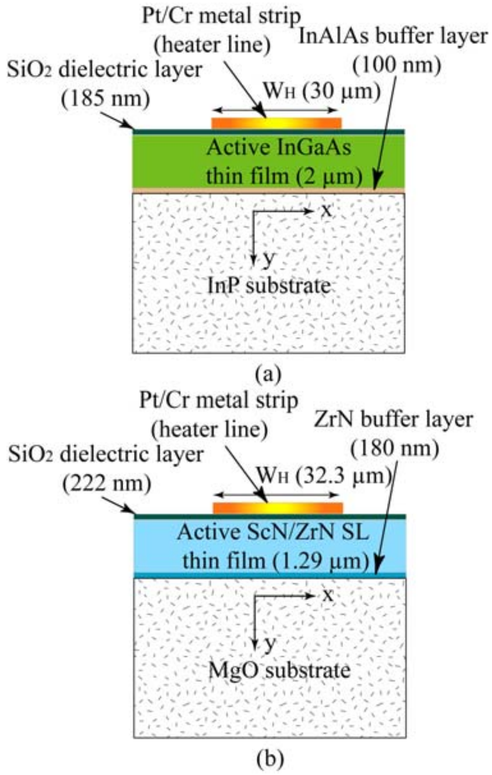

Figure 1: Schematic diagram of the two test structures studied; the isotropic InGaAs thin film on the isotropic InP substrate (a), and the anisotropic ScN/ZrN superlattice thin film on the isotropic MgO substrate (b).

The metal heater in the first sample is 30 µm wide, which is 15 times greater than the thickness of the top InGaAs semiconductor film. Additionally, the thermal conductivity of the top InGaAs film is expected to be much smaller than the thermal conductivity of InP. As discussed by many authors [1-6], under these conditions for low frequencies (<1kHz) the thin film can be modeled as thermal resistance. This resistance shifts the temperature distribution by a constant factor that is independent of the frequency of excitation of the heater, and given by:

$$\Delta T_f(x) = \Delta T_T(x) - \Delta T_S(x) = \frac{P}{l}\frac{d_f}{W_H \beta_f} \quad (1)$$

where $\Delta T_T(x)$, is the temperature distribution of the combined thin film and substrate, and $\Delta T_S(x)$ is the distribution of the substrate alone. P/l is the amplitude of the power per unit length generated at frequency 2ω in the heater. d_f and β_f are the thickness and the thermal conductivity of the semiconductor thin film, respectively, and W_H is the width of the metal heater strip.

The characteristic length of temperature oscillations is given by the thermal penetration depth of the InP substrate q_S^{-1} defined by [1]:

$$q_S^{-1} = \sqrt{\frac{\alpha_S}{2i\omega}} \quad (2)$$

In the low frequency range (<1kHz) the thermal penetration depth of the InP substrate is very large compared to the metal heater strip width. Under these conditions the latter can be approximated as an infinitely narrow line.

The temperature oscillation at a distance x from an infinitely narrow line heat source on the surface of a semi-infinite substrate is given by [7]:

$$\Delta T_S(x) = \frac{P}{l\pi\beta_S} K_0(q_S x) \quad (3)$$

where K_0 is the zeroth-order modified Bessel function and β_S is the thermal conductivity of the substrate.

In figures 2 (a) and (b), we have plotted the modulus and phase of $\frac{\Delta T_T(x)}{P/l}$ as a function of distance from the line heat source for excitation frequencies ω = 5, 30, and 106 Hz.

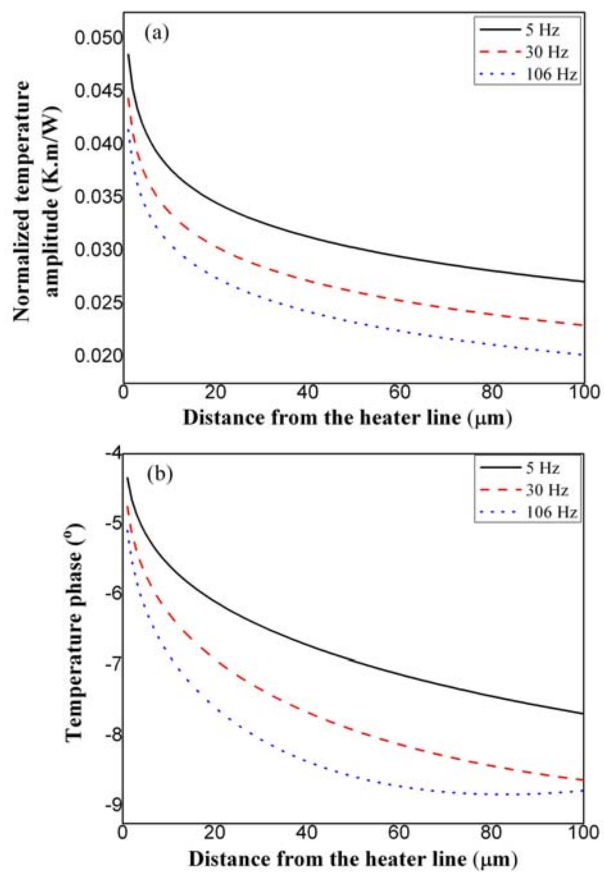

Figure 2: Simulated temperature amplitude (a) and phase (b) as a function of distance from the heater line for different frequencies, in the case of anisotropic thin film on top of an isotropic semi-infinite substrate.

2.2. Application of thermoreflectance to extract thermal conductivity

With the temperature distributions provided by thermal images, thermal conductivity can be determined by comparing the ratio of temperatures for two points at known distances perpendicular to the heater. To demonstrate the concept, we consider two cases involving samples with isotropic thermal conductivity. In the first, ideal, case we model the heat source as infinitely narrow line on the surface of a semi-infinite substrate. In the second case we include the effect of thin semiconductor film on top of a semi-infinite substrate and give the heater a finite width W_H.

For both cases, we assume the frequency range for which the thermal penetration depth q_S^{-1} would be very large $q_S^{-1} >> W_H$, and we are interested in an area much smaller than a disc with radius q_S^{-1}.

In the first case the temperature distribution on the surface is given by [1]:

$$\Delta T(x) = \frac{P}{l\pi\beta_S}\left\{\ln\left[\frac{2}{x}\sqrt{\frac{\alpha_S}{2\omega}}\right] - E_C - i\frac{\pi}{4}\right\} \qquad (4)$$

where E_C=0.5772 is the Euler constant. If we take the ratio of the real part of equation (4) on two different points x_1 and x_2 at the vicinity of the metal heat line, we will have:

$$\frac{\mathrm{Re}[\Delta T(x_1)]}{\mathrm{Re}[\Delta T(x_2)]} = \frac{\mathrm{Re}\left[\frac{\Delta R}{R}(x_1)\right]}{\mathrm{Re}\left[\frac{\Delta R}{R}(x_2)\right]} = \frac{\ln\left[\frac{2}{x_1}\sqrt{\frac{\alpha_S}{2\omega}}\right] - E_C}{\ln\left[\frac{2}{x_2}\sqrt{\frac{\alpha_S}{2\omega}}\right] - E_C} = \varepsilon \qquad (5)$$

After some algebra, it is very easy to get the expression of the thermal diffusivity of the substrate:

$$\alpha_S = \frac{\exp(2E_C)}{2}\omega\left(\frac{x_1}{x_2^{\varepsilon}}\right)^{\frac{2}{1-\varepsilon}} \qquad (6)$$

Therefore the thermal properties of the thin film can be obtained from the real part of the thermoreflectance response at two locations on the film's surface. Note that because the power terms cancel, the calculation uses the thermoreflectance change on the surface and not the actual temperature. Therefore it is not necessary to calibrate for the thin film's thermoreflectance coefficient. In the second case, by neglecting the thermal resistances at the different interfaces, the temperature distribution on the surface under the assumptions made above, is given by [2, 3, 4]:

$$\Delta T(x) = \frac{P}{l}\left\{\frac{1}{\pi\beta_S}\left[\ln\left(\frac{2}{x}\sqrt{\frac{\alpha_S}{2\omega}}\right) - E_C - i\frac{\pi}{4}\right] + \frac{d_f}{\beta_f W}\right\} \qquad (7)$$

The same procedure as above plus some algebra allows us to get the expression of the thermal conductivity of the thin film as:

$$\beta_f^{-1} = \frac{W}{\pi\beta_S d_f}\left\{\ln\left[\sqrt{\frac{2\omega}{\alpha_S}}\left(\frac{x_1}{x_2^{\varepsilon}}\right)^{\frac{1}{1-\varepsilon}}\right] + E_C - \ln(2)\right\} \qquad (8)$$

2.3. Measurement of the thermal conductivity anisotropy

Recently very sophisticated analysis has been developed to improve the 3ω method to be able to extract simultaneously the thermal conductivity, heat capacity, thermal conductivity anisotropy, and interlayer contact resistance in the general case of multilayer anisotropic structures [4, 5]. The two-dimensional analytical solution derived by Borca-Tasciuc et al [4] for the complex temperature distribution on the surface of multilayer structures with anisotropic thermophysical properties is one of the main results obtained to date using the 3ω technique.

Material anisotropy is especially sensitive to experimental conditions since it can only be detected by heat motion that is strongly two-dimensional. Figure 3 shows how the linewidth of the metal heater strip can influence the heat flow path [5].

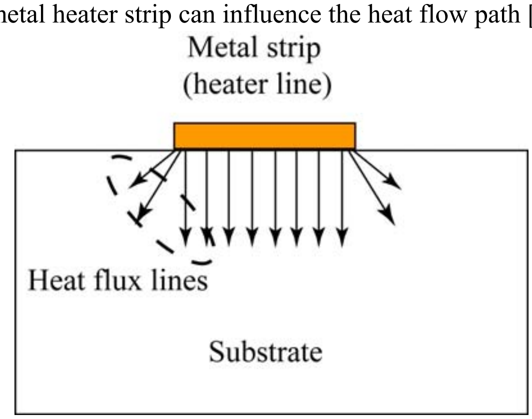

Figure 3: A sketch illustrating the effect of width of the metal heater strip on the heat flux path in a 3ω system.

In previous work, Borca-Tasciuc et al [4] used an iterative method using two metal heater strips of different width deposited on the same sample to extract the thermal conductivity anisotropy of thin film nanochanneled alumina. Thermoreflectance imaging has the advantage of acquiring the temperature distribution over a large surface area including the metal heater strip and vicinity in a single measurement. Starting from equation (1) of reference [4], we can show that the complex temperature distribution on the surface of a multilayer anisotropic structure would be given by:

$$\Delta T(x) = -\frac{P}{\pi l\beta_{y1}}\int_0^{\infty}\frac{\sin(kb)}{kb}\frac{\cos(kx)}{A_1 B_1}dk \qquad (9)$$

where β_{y1} is the cross-plane thermal conductivity of the nominal thin film, A_1 and B_1 are as defined in reference [4], and b is the metal heater half-width $W_H/2$. The temperature distribution on the thin film very close to the heater edge would be sensitive to both the cross-plane and the in-plane components of its thermal conductivity. Using thermoreflectance imaging we can get the temperature profile at any frequency in the vicinity of the metal heater. Then, under the assumption of knowing the thermal properties of the substrate, it is easy to fit the experimental temperature profile using equation (9) and optimize the remaining free parameters to obtain the in-plane and cross-plane components of the thermal conductivity of the thin film.

As shown above, even in this general case, the thermoreflectance method does not need to know the amplitude of the power per unit length *(P/l)* in the heater. This term cancels when taking the ratio of temperatures in the vicinity of the metal heater.

3. Experiment

Figure 4 below shows a schematic diagram of the experimental set up used in the thermoreflectance imaging technique.

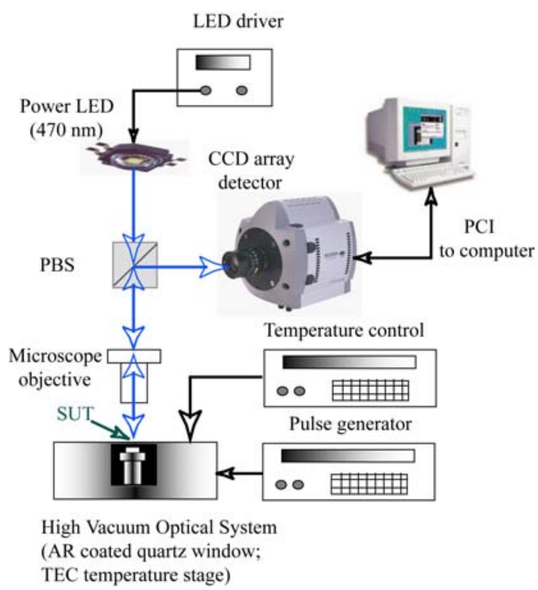

Figure 4: Schematic diagram of the experimental set-up used in the thermoreflectance imaging technique.

Thermoreflectance imaging is a proven and quick way to obtain temperature distributions on active devices. The optical, non-contact method can obtain two-dimensional thermal maps with submicron spatial resolution and 5-50 mK temperature resolution. This is accomplished by measuring the temperature dependent reflectivity change at material interfaces. References [8-12] provide a survey of thermoreflectance imaging techniques.

4. Results and discussion

Figure 5 (a) shows a thermoreflectance image of the heater line on top of the isotropic InGaAs thin film for an electrical excitation at 5 Hz. The relative change of reflectivity ($\Delta R/R$) decreases as a function of distance away from the heater line. Figures 5 (b) and (c) show the amplitude and phase profiles for the isotropic InGaAs sample obtained from thermoreflectance imaging at 5, 30, and 106 Hz. Profiles are taken along the perpendicular axis to the heater line as shown in figure 5 (a). There is close agreement between the prediction of eq. 3 plotted in figures 2 and the experimentally obtained profiles.

To extract the thermal conductivity of the isotropic InGaAs thin film according to equation (7), the main condition is to ensure very large thermal penetration depth within the InP substrate. This condition is met at low excitation frequency. For this reason, we chose the amplitude profile data at 5 Hz to extract thermal conductivity. Figure 5 (d) shows the thermoreflectance distribution after noise removal.

As we have seen in section 2, the thermal conductivity of an isotropic thin film on top of an isotropic semi-infinite substrate is determined from the ratio of the real part of temperatures at different locations along the profile.

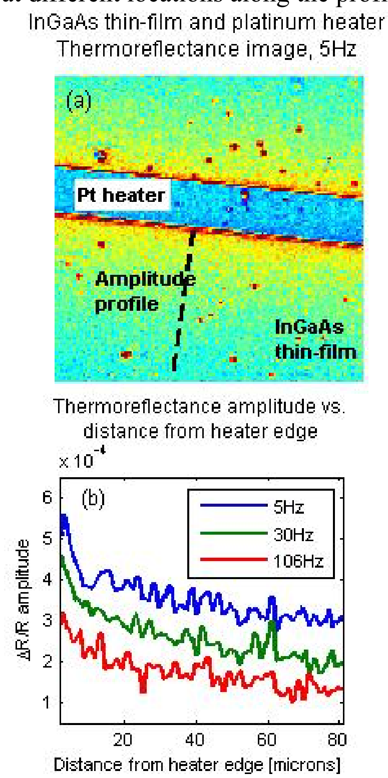

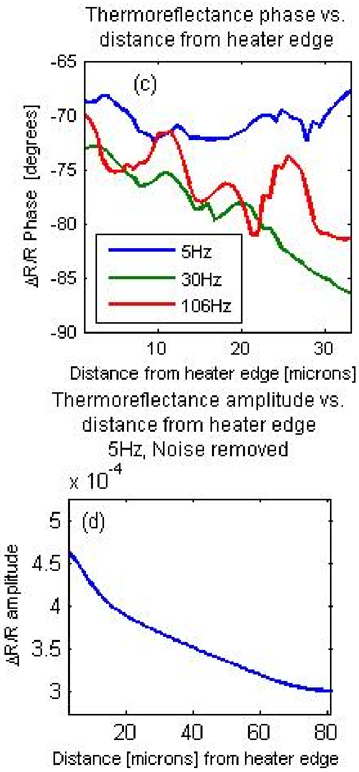

Figure 5: (a) Thermoreflectance image of the heater line on top of the InGaAs thin film sample. ΔR/R amplitude (b) and phase (c) profiles perpendicular to heater for frequencies 5, 30, and 106 Hz. Smoothed ΔR/R amplitude profile at 5 Hz.

The relative change of reflectivity ΔR/R is proportional to the temperature, and the coefficient of proportionality is called thermoreflectance coefficient [8-12].

Application of equation (8) for different point pairs along the curve of figure 5 (d) resulted in a thermal conductivity for the InGaAs thin film $\beta_f \approx 4.1$ W/m/K within 30% error. The origin of this high error is due to the noise level in the thermoreflectance image data, caused by the low overall reflectivity of the thin film and the roughness of the sample surface. Other approximations made in the theoretical background could be source of error too. Using this value of β_f in combination with a scaling factor, the simulated curve based on equation (7) is a close fit to the experimental curve represented in figure 5 (d). The value found for β_f is in good agreement with the one extracted using 3ω method [13].

The active thin film in the second test structure we have studied is a 1.29 μm ScN/ZrN metal superlattice. The thin film is grown on an isotropic thermally thick MgO substrate. They are separated by a 180 nm ZrN buffer layer. The metal heater strip is deposited on top of the structure and electrically isolated from the thin film superlattice by a 222 nm SiO_2 layer. A schematic diagram of the structure is illustrated in figure 1 (b). The artificial stratified structure of the superlattice gives rise to anisotropic thermal properties.

As we have shown in section 2, theoretically it is possible to extract both the in-plan and cross-plan components of the thermal conductivity of the thin film using the complete equation (9) or simplified expression of it. The input experimental data would be two profiles of the real parts of ΔR/R for two different frequencies.

Unfortunately, thermoreflectance profiles of sufficient signal to noise were not obtained in time for this report. The detail of application of thermoreflectance imaging to the extract of the thermal conductivity anisotropy of thin films will be presented in a future work.

5. Conclusions

We have proposed thermoreflectance imaging as an alternate method to 3ω for extracting thermal conductivity in thin films and bulk materials. The method is valid for materials with either, isotropic or anisotropic in-plane and cross-plane thermal conductivities. By working exclusively from the thermoreflectance distribution in the thermal image, the method is less sensitive to the electrical properties of the heat source. We have shown also that calibration and absolute temperature values are not required in order to determine the thin film thermal conductivity.

Acknowledgments

The authors would like to thank Professor Arum Majumdar of UC Berkeley and his students for providing the test samples used in this study.

References

1. D. G. Cahill, Rev. Sci. Instrum, **61**, 802, (1990).
2. S. M. Lee and D. G. Cahill, J. Appl. Phys, **81**, 2590, (1997).
3. J. H. Kim, A. Feldman, and D. Novotny, J. Appl. Phys, **86**, 3959, (1999).
4. T. Borca-Tasciuc, A. R. Kumar, and G. Chen, **72**, 2139, (2001).
5. B. W. Olson, S. Graham, and K. Chen, Rev. Sci. Instrum, **76**, 053901, (2005).
6. T. Tong and A. Majumdar, Rev. Sci, Instrum, **77**, 104902, (2006).
7. H. S. Carslaw and J. C. Jaeger, *Conduction of Heat in Solids* (Oxford University Press, Oxford, 1959).
8. S. Dilhaire, S. Grauby, and W. Cleays, Appl. Phys. Lett, **84**, 822, (2004).
9. P. E. Raad, et al
10. G. Tessier et al
11. James Christofferson and Ali Shakouri, "Thermoreflectance based thermal microscope", Review of Scientific Instruments, 76, 024903-1-6, Jan., (2005).
12. Christofferson, J.; Vashae, D.; Shakouri, A.; Melese, P.; Xiaofeng Fan; Gehong Zeng; Labounty, C.; Bowers, J..E.; Croke, E.T., III, “Thermoreflectance imaging of superlattice micro refrigerators,” Seventeenth Annual IEEE Semiconductor Thermal measurement and Management Symposium, San Jose, CA, USA, 20-22 March (2001).
13. W. Kim, J. Zide, A. Gossard, D. Klenov, S. Stemmer, A. Shakouri, and A. Majumdar, Phys. Rev. Lett, **96**, 045901, (2006).